



Twin boundary characters established during dynamic recrystallization in a nickel alloy



Hui Shi ^{a,b}, Ke Chen ^{a,b,*}, Zhi Shen ^c, Jieqiong Wu ^{a,b}, Xianping Dong ^{a,b}, Lanting Zhang ^{a,b}, Aidang Shan ^{a,b}

^a Shanghai Key Lab of Advanced High-Temperature Materials and Precision Forming, Shanghai Jiao Tong University, 800 Dongchuan Road, Shanghai 200240, China

^b School of Materials Science and Engineering, Shanghai Jiao Tong University, 800 Dongchuan Road, Shanghai 200240, China

^c Shanghai Electric Power Generation Equipment Co., Ltd., 333 Jiangchuan Road, Shanghai 200240, China

ARTICLE INFO

Article history:

Received 25 June 2015

Received in revised form 11 October 2015

Accepted 14 October 2015

Available online 21 October 2015

Keywords:

Twin boundary

Dynamic recrystallization

Nickel alloy

EBSD

ABSTRACT

For the purpose of providing fundamentals for grain boundary engineering design for high-temperature alloys, twin boundary characters are studied quantitatively in a nickel alloy during DRX to improve the understanding of twin boundary evolution during hot deformation. The nickel alloy samples were hot compressed at temperatures of 1120–1180 °C and strain rates of 0.1 s⁻¹ and 1 s⁻¹ to a fixed true strain of 1.1. Refined equiaxed grain structure is obtained with abundant twin boundaries. Most of the twin boundaries form inside the grains, being highly coherent and showing rather limited mutual interaction. An inversely proportional relationship is found between $\Sigma 3$ twin boundary length density (BLD _{$\Sigma 3$}) and DRX grain size (D_{DRX}). An analytical model is derived here, in good agreement with current experimental results, indicating that the stored strain energy difference across grain boundary is the main driving force for grain boundary migration and determines the annealing twin formation during DRX. $\Sigma 3$ twin boundary length density (BLF _{$\Sigma 3$}) developed in DRX was found varying within a small range of 44%–48%, which is shown to result from the inverse proportionality between grain boundary length density (BLD_{GB}) and D_{DRX} as well as the inverse proportionality between BLD _{$\Sigma 3$} and D_{DRX} .

© 2015 Elsevier Inc. All rights reserved.

1. Introduction

An increased interest in annealing twin has been aroused by the concept of grain boundary engineering, the aim of which is to improve material properties against intergranular degradation by promoting fraction of special boundaries and tailoring grain boundary character distribution (GBCD) [1,2]. Since the initial proposition of grain boundary design by Watanabe in 1984 [3], much attention has been paid to this field with many successful applications of grain boundary engineering to FCC materials of low stacking fault energy through improving material properties like strength, creep/rupture life, corrosion resistance, fatigue [4–8]. Although controversy still exists when it comes to the definition and category of ‘special boundary’, $\Sigma 3$ twin boundary and related $\Sigma 3^n$ boundaries have been proved to be mainly responsible for improved properties of grain boundary engineered materials of FCC structure [1,9].

Most of the established thermomechanical processing routes for grain boundary engineering contain multiple cycles of cold deformation and subsequent annealing [1,2]. However, for materials like nickel-based superalloys that are normally processed at elevated temperatures, few systematic studies have been carried out and no mature processing route has been established. Bozzolo and Souai investigated the dependence of

annealing twin formation on processing parameters during hot deformation and demonstrated the possibility of grain boundary engineering via hot working in a nickel-base superalloy [10,11]. However, existing knowledge is far from sufficient on the underlying mechanisms of the twin boundary generation and evolution during grain boundary engineering. Moreover, most researches concerning annealing twin density evolution focused on the static processes like recrystallization and grain growth with few attention on annealing twin established in DRX [12–17]. Both the formation mechanism of annealing twin boundaries and the rule governing twin boundary evolution under various thermomechanical processes are still controversial and insufficient. In addition, twin boundary characters established in DRX has been rarely studied in a systematic way, which limits the development of grain boundary engineering for high-temperature alloys. Thus, it is essential to investigate the twin boundary formation and evolution during DRX to assist in the design of grain boundary engineering routes for high-temperature alloys.

In the current research, twin boundary characters and their evolution have been studied quantitatively in detail in the process of DRX during hot deformation for the first time to our knowledge. The quantity of $\Sigma 3$ twin boundaries was quantified both in boundary length fraction (BLF), defined as the length fraction of $\Sigma 3$ twin boundaries among all boundaries with misorientation higher than 15° (BLF _{$\Sigma 3$} , %), and in boundary length density (BLD), defined as the length of $\Sigma 3$ twin boundaries per unit area (BLD _{$\Sigma 3$} , μm^{-1}). BLF _{$\Sigma 3$} is of great importance to grain boundary engineering because it is relevant to the extent of grain

* Corresponding author at: 407 Material Building A, 800 Dongchuan Road, Shanghai 200240, China.

E-mail address: chenke83@sjtu.edu.cn (K. Chen).

boundary network breakup [1], while $BLD_{\Sigma 3}$ is more frequently used to investigate the factors governing the twin boundary density evolution [12,15]. Our study intends to make a thorough investigation of twin boundary characters established during DRX, in order to improve the understanding on formation and evolution of twin boundaries under various hot deformation conditions, thus providing a solid foundation for grain boundary engineering design for high-temperature alloys.

2. Materials and methods

Nimonic 80A was supplied by Baosteel in the form of forged cylindrical rod with an average grain size of 30 μm . The as-received material was solution treated at 1065 $^{\circ}\text{C}$ for 8 h and then water quenched to room temperature. The initial microstructure before hot compression is shown in Fig. 1. After solution treatment, the average grain size increased to 170 μm and the microstructure is rather homogeneous (Fig. 1a). High angle boundary network is severely interrupted by $\Sigma 3^{\text{n}}$ clusters containing interconnected $\Sigma 3$, $\Sigma 9$ and $\Sigma 27$ boundaries, as shown in Fig. 1b. $BLF_{\Sigma 3}$ is over 70% and $BLD_{\Sigma 3}$ is 0.035 μm^{-1} . During hot compression conducted in the current study, DRX occurred and the original boundaries were swept out in the process of formation and growth of new grains.

Hot compression tests were carried out on a Gleeble 3500 system at temperatures of 1120–1180 $^{\circ}\text{C}$ and strain rates of 0.1 s^{-1} and 1 s^{-1} to a fixed true strain of 1.1. The samples were heated at the rate of 5 $^{\circ}\text{C}/\text{s}$ until the deformation temperature was reached and then retained at deformation temperature for 3 min before they were stressed. After stressing, the samples were water quenched to room temperature to freeze the high temperature microstructures at the cooling rate of around 120 $^{\circ}\text{C}/\text{s}$. The temperature range was selected to cohere with the industrial forging process. Since the deformation temperature is much higher than the γ' solvus temperature, the influence of γ' phase during hot deformation is negligible [18,19]. Steady stage of DRX was reached in the central region in all samples. Cylindrical specimens after hot deformation were sectioned symmetrically into two parts along the compression axis at the geometric center. Then specimens were ground and mechanically polished, and finished by a final polish using 0.05 μm colloidal silica.

Electron backscattered diffraction (EBSD) technology was used for quantitative analyses on grain structure and grain boundary characters. EBSD measurements were carried out using a FEI NOVA NanoSEM 230 scanning electron microscope (SEM) equipped with Advanced Fast EBSD detector at an accelerating voltage of 20 kV. The step size was set to be 0.5 μm for strain rate 1 s^{-1} and 1 μm for strain rate 0.1 s^{-1} according to the grain sizes. All the data was analyzed from at least two maps obtained from different regions comprising at least 400 grains.

For grain reconstruction in EBSD analyses, the grain is defined as a region being completely bounded by boundaries whose misorientation angles exceed 15 $^{\circ}$, excluding $\Sigma 3$ twin boundaries. The identification of $\Sigma 3$ twin boundaries and $\Sigma 9$ boundaries is based on the Brandon criterion [20]. Due to significant difference between coherent twin boundary (CTB) and incoherent twin boundary (ITB), it is necessary to provide additional differentiation. However, since the two degrees of freedom associated with the boundary plane are not readily given by 2-D EBSD scans, it is impossible to determine the coherency of $\Sigma 3$ twin boundaries directly. Trace analysis has shown good reliability, in which the alignment between the trace of the boundary plane and the trace of the twinning plane is assessed. $\Sigma 3$ boundaries deviating by less than 5 $^{\circ}$ from the trace of the closest {1 1 1} plane are considered to be coherent, others regarded as incoherent [10]. The differentiation can be readily carried out by OIM analysis software. $\Sigma 3$ and $\Sigma 9$ boundaries were quantified on the basis of both BLD and BLF in the current study.

3. Results

3.1. Grain structure evolution

Figs. 2 and 3 show the grain structure and grain boundary characters (both including and excluding $\Sigma 3$ twin boundaries) of samples deformed at strain rates of 1 s^{-1} and 0.1 s^{-1} , respectively. The grain structures obtained after hot deformation are almost equiaxed and rather homogeneous indicating of unimodal grain size distribution. Unlike the grain shape and grain size distribution, grain size varies depending on the deformation temperature and strain rate. With increasing temperature, the grain structure coarsens at both strain rate of 1 s^{-1} (Fig. 2) and 0.1 s^{-1} (Fig. 3). At the same temperature, the grain structure developed at 1 s^{-1} is finer than that at 0.1 s^{-1} (comparison between Figs. 2 and 3).

Grain structure obtained in DRX is highly twinned with twin boundaries mostly straight and existing inside of the grains, which is in good agreement with the twin morphology and distribution obtained in DRX by Mandal et al. [21]. The EBSD grain boundary maps excluding twin boundaries also clearly show that twin boundaries formed in DRX are not involved in the general high angle grain boundary network. In addition, $\Sigma 9$ boundaries (colored in green) can be identified as short individual segments connected to $\Sigma 3$ twin boundaries and the quantity of $\Sigma 9$ boundaries is very low compared with $\Sigma 3$ twin boundaries.

Fig. 4 reveals the DRX grain size (D_{DRX}) variation with deformation temperature and strain rate. As demonstrated by other studies [22,23], D_{DRX} decreases with increasing the value of Zener–Hollomon parameter ($Z = \dot{\epsilon} \exp(Q/RT)$), that is, D_{DRX} decreases with increasing strain rate

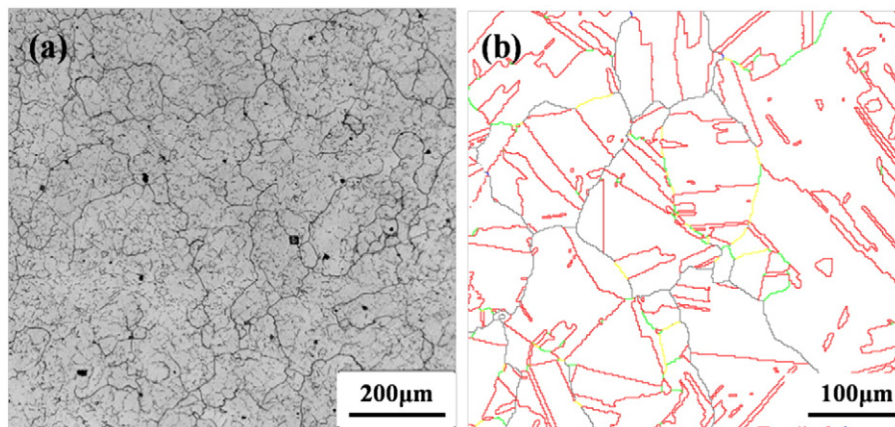


Fig. 1. Initial microstructure of Nimonic 80A before hot compression: (a) Optical metallograph, and (b) EBSD grain boundary map. ($\Sigma 3$ twin boundaries are shown as red lines, $\Sigma 9$ boundaries shown as green lines, $\Sigma 27$ boundaries shown as yellow lines and high-angle boundaries ($>15^{\circ}$) shown as black lines).

Download English Version:

<https://daneshyari.com/en/article/1570683>

Download Persian Version:

<https://daneshyari.com/article/1570683>

[Daneshyari.com](https://daneshyari.com)